

# Ibn Al-Haitham Journal for Pure and Applied Sciences

Journal homepage: jih.uobaghdad.edu.iq PISSN: 1609-4042, EISSN: 2521-3407 IHJPAS. 2025, 38(4)



# Study of Nuclear Deformations for Some Nuclei located Near the Nuclear Island of Inversion Region

Luay F. Sultan¹\*<sup>®</sup> and Ali A. Alzubadi <sup>2</sup>®

<sup>1,2</sup>Department of Physics, College of Science, University of Baghdad, Baghdad, Iraq. \*Corresponding Author

Received: 21 April 2025 Accepted: 24 July 2025 Published: 20 October 2025

doi.org/10.30526/38.4.4146

#### **Abstract**

In this work, we have carried out a detailed theoretical analysis of the nuclear deformations of some of the nuclei situated in the vicinity and within the nuclear Island of Inversion. The properties that were studied included the calculation of the magnetic moment and the electric quadrupole moment to gather with reduced quadrupole deformation parameter for even-even isotopes of Ne, Mg, and Si nuclei, to explain the behavior of the nuclei in question, and how much they deviate from the spherical shape in this critical region. All theoretical computations were conducted utilizing the NushellX@MSU shell model code within the sd space with the effective two-body interaction USDC. The comparative analysis with available experimental data revealed that certain theoretical parameterizations produced results in good agreement with experimental values. For instance, the theoretical magnetic moment of  $^{29}$ Si was found to be -0.522, closely matching the experimental value of -0.555, indicating reasonable consistency. Furthermore, noticeable variations were observed in the calculated moments and deformations of the studied nuclei. For example, <sup>31</sup>Mg exhibited a theoretical magnetic moment of 1.348 compared to the experimental value of -0.883. Additionally, some isotopes displayed very large deformations, which confirms the presence of intricate shell effects due to the increased number of neutrons and the resulting modifications in the internal structure of the nucleus.

**Keywords:** Magnetic moment, electric quadrupole, island of inversion, reduced quadrupole deformation parameter.

#### 1.Introduction

The study of these nuclear moments becomes more relevant due to the understanding of the nuclear structure associated with exotic or neutron-rich nuclei. The study of magnetic dipoles and electric quadrupoles of nuclei provides an insight into the evolution of shells within nuclei and the fundamental forces, as well as the deformation patterns of the considered unstable nuclei (1). These studies help improve the models, especially in the rejection region close to the nuclear island of inversion (NIOI) (2). Among the nuclear moments important for understanding the structure of the nucleus and providing information regarding the shape and charge distribution of the nucleus, the electric quadrupole moment and magnetic dipole moment rank as the most important (3).

The magnetic dipole moment of a nucleus is determined by the orbits of nucleons in the nucleus, their distribution, and their interaction with different energy levels. On the other hand, the electric quadrupole moment describes the change of the charge distribution within the nucleus and is also a fundamental measure of how much the nucleus deviates from a spherical shape to prolate or oblate shapes (4). Here, the shell model gives one of the most basic accounts of the magnetic and electric moments (5). In this model, the nuclei are regarded as shells counterparts of atoms, that is, nucleons are believed to form shells about the nucleus. The nucleus is assumed to have a balance for the orbital motion of nucleons and the forces they apply to each other. This model fails for spin-orbit shells that have a large number of valence nucleons. This is because the moments that are dominated by strong interactions between a few outer nucleons result in a different effective nuclear moment than would be obtained if realistic but naive models were employed (6). This needs to extend the model to incorporate the collective influences of the nucleus. Considered one of the most fascinating areas in the studies of nuclear structure, the Nucleus Island of Inversion (NIOI) is characterized on the one hand by extreme changes (striking) in energies of shells (energy levels) into which nucleons are grouped (7). In this area, some nuclei formerly considered stable show unusual behaviors such as observations of inversions in the ordering of orbitals of nucleons (8). This gives rise to changes of remarkably large magnitude in their electric and magnetic moments, providing opportunities for intensive research on the effects of interactions between nucleons within this structure.

Skyrme-Hartree-Fock (SHF) theory is a fundamental theoretical framework for nuclear structure. It describes nucleon interactions in terms of Skyrme parameters using effective potentials and allows nuclear energy levels and density distributions to be calculated with high precision. In use as a single-particle potential, the SHF model provides a simple and useful description of central and spin-orbit interactions, which govern nucleon dynamics. It can be applied to static and dynamic nuclear properties, e.g., neutron-rich nuclei separation and deformation energies 9).

Among the previous studies on this region, (10) evaluated the electric quadrupole moment and magnetic moment of <sup>32</sup>Al (Z=13, N=19). Both of the moments were found to be well described by full SD shell model calculations with USD effective interaction. These results were a definite proof that <sup>32</sup>Al did not belong to the nuclear island of inversion. The study (11) pointed of even–even isotopes of Ne, Mg, Si, S, Ar, and Kr as a system using the Hartree–Fock–Bogoliubov approach with the SLy4 Skyrme parameterization, considering nuclear deformation. It was made a more detailed study of nucleon interactions in the NIOI and their bearing on the magnetic and electric moments, concentrating on the developments around N=20 (12).

In this study, we shall calculate the magnetic dipole ( $\mu$ ) and electric quadrupole moments  $Q_2$ ) along with the reduced quadrupole deformation parameter ( $\beta_2$ ) for Si, Mg, and Ne isotopes within the nuclear island of inversion (NIOI) region. This work was carried out using the shell model approach, which incorporates the two-body effective interactions with the single-particle potential. To achieve this, the *SD shell model space* was adopted.

#### 2.Materials and Methods

The electric  $2^L$  pole operator  $r^*r^LY_{LM}(\hat{r})$  has parity  $(-1)^L$ , so the electric  $2^L$  pole moment must vanish for odd L. The intrinsic is defined in respect to the symmetry axis of the charge distribution. The sum of products of one body density matrix element (OBDM) and single-particle matrix elements gives the nuclear matrix element corresponding to the

electromagnetic  $(\hat{O})$  and electron scattering  $(\hat{T})$  operators for initial (I) and final (f) nuclear states, with some multipolarity (13):

$$\langle f \| \hat{X}(\lambda)_{t_z} \| i \rangle = \sum_{k_a k_b} OBDM(fik_a k_b \lambda) \langle k_a \| \hat{X}(\lambda)_{t_z} \| k_b \rangle \tag{1}$$

The operator  $(\hat{X})$  encompasses both the electron scattering operator  $(\hat{T})$  and electromagnetic operator  $(\hat{O})$ . k denotes single-particle states (nlj) the OBDM is found as follows:

$$OBDM(fik_ak_b\lambda) = \frac{\langle f | \left[ a_{k_a}^+ + \otimes \tilde{a}_{k_b} \right]^{\lambda} | i \rangle}{\sqrt{2\lambda + 1}}$$
 (2)

All of the quantum numbers necessary to distinguish the states are incorporated into (I) and (f). As defined by the M1 operator, so the magnetic dipole moment  $(\mu)$  is given by (14):

$$\mu = \sqrt{\frac{4\pi}{3}} \begin{pmatrix} J & J & J \\ -J & 0 & J \end{pmatrix} \sum_{t_z} \langle J \| \hat{O}(M1)_{t_z} \| J \rangle \mu_N \tag{3}$$

Where the operator of the magnetic transition is  $\langle J \| \hat{O}(M1)_{t_z} \| J \rangle$ , and the nuclear magneton is  $\mu_N$ , where  $\mu_N = \frac{e\hbar}{2m_pc} = 0.1051$  efm, with the  $m_p$  proton mass. The orbital as well as spin free nucleon g factors g(free) are:  $g_l^p = 1$ ,  $g_s^p = 5.585$ , for proton and  $g_l^p = 0$ ,  $g_s^p = -3.826$  for neutron (14).

According to the E2 operator, can defined the electric quadrupole moment (Q) as:

$$Q = \sqrt{\frac{16\pi}{5}} \begin{pmatrix} J_i & 2 & J_i \\ -J_i & 0 & J_i \end{pmatrix} \sum_{t_z} \langle J \| \hat{O}(E2)_{t_z} \| J \rangle e_{t_Z}$$

$$\tag{4}$$

The Skyrme potential is used for the central potential; it is composed of two-body interactions. One-body potentials can be formulated within the Hartree-Fock (HF) approximation framework (15). This is a mean-field potential that serves to approximate the true interactions of the nucleon-nucleon (and nucleon-triple N) systems through a mean-field constructed from all of the nucleons in the nucleus. The potential  $V_{Skyrme}$  is written as follows (16):

$$V_{Skyrme} = t_{0} \left( 1 + x_{0} \hat{P}_{\sigma} \right) \delta_{12} + \frac{t_{1}}{2} \left( 1 + x_{1} \hat{P}_{\sigma} \right) \left[ \vec{k}^{2} \delta_{12} + \delta_{12} \vec{k}^{2} \right] + t_{2} \left( 1 + x_{2} \hat{P}_{\sigma} \right) \vec{k}^{2} \delta_{12} + \frac{t_{3}}{6} \left( 1 + x_{3} \hat{P}_{\sigma} \right) \rho \left( \frac{\vec{r}_{1}, \vec{r}_{2}}{2} \right) \delta_{12} + i W_{0} \vec{k}^{2} \delta_{12} \left( \vec{\hat{\sigma}}_{1} + \vec{\hat{\sigma}}_{2} \right) \times \vec{k} + \frac{t_{2}}{2} \left( \left[ 3 \left( \vec{\hat{\sigma}}_{1}, \vec{k}^{2} \right) \left( \vec{\hat{\sigma}}_{2}, \vec{k}^{2} \right) - \left( \vec{\hat{\sigma}}_{1}, \vec{\hat{\sigma}}_{2} \right) \vec{k}^{2} \right] \delta_{12} + \delta_{12} \left[ 3 \left( \vec{\hat{\sigma}}_{1}, \vec{k} \right) \left( \vec{\hat{\sigma}}_{2}, \vec{k} \right) - \left( \vec{\hat{\sigma}}_{1}, \vec{\hat{\sigma}}_{2} \right) \vec{k}^{2} \right] \right) + t_{0} \left[ 3 \left( \vec{\hat{\sigma}}_{1}, \vec{k} \right) \delta_{12} \left( \vec{\hat{\sigma}}_{2}, \vec{k} \right) - \left( \vec{\hat{\sigma}}_{1}, \vec{\hat{\sigma}}_{2} \right) \vec{k}^{2} \delta_{12} \vec{k} \right] \right]$$

$$(5)$$

Where  $\delta_{12} = \delta(\vec{r_1} - \vec{r_2})$  and k, k' are the relative momentum operators, k acting from right and k' acting on the left and are given by:

$$\vec{\mathbf{k}}' = -\frac{1}{2i} (\vec{\nabla}_1 - \vec{\nabla}_2), \vec{\mathbf{k}} = \frac{1}{2i} (\vec{\nabla}_1 - \vec{\nabla}_2)$$
 (6)

also, the operator of the spin-exchange  $\widehat{P}_{\sigma}$  is given as:

$$\widehat{P}_{\sigma} = \frac{1}{2} (1 + \widehat{\sigma}_1 \cdot \widehat{\sigma}_2) \tag{7}$$

Where  $\hat{\sigma}_1$ ,  $\hat{\sigma}_2$  are the Pauli spin matrices

Calculation of the reduced quadrupole deformation parameter is also presented for the isotopes considered in this work, which is defined as (17).

$$\beta_2 = 4\pi [B(E2); 0_1^+ \to 2_1^+]^{1/2} / (ZR_0^2 e), \text{ where } R_0 = 1.2A^{1/3}$$
 (8)

#### 3. Results and Discussion

NushellX@MSU (18) shell model code was applied in the theoretical computations of the Si, Mg, and Ne nuclei within the island of inversion region of the nuclear shell for the magnetic dipole moment, electric quadrupole moment, and reduced quadrupole deformation parameter as an example. The radial wave functions corresponding to the single particle matrix elements were calculated using a two-body Skyrme interaction potential. Supporting tables and figures will be provide along with the discussion of the results.

#### 3.1. The Magnetic Dipole Moment

Utilizing the USDC two-body effective interactions, we have calculated the magnetic dipole moments of the aforementioned isotopes within the sd model space. The computed values are shown in **Table 1** alongside the respective measured values from (19). The information presented earlier seems to justify the assertion that the computed magnetic dipole moments, pertaining to the isotopes in question, concordantly somewhat agree with the experimental evidence accessible in (19).

**Table 1.** Comparison of the theoretical calculation of magnetic dipole moments  $\mu$  (nm) for isotopes Si, Mg, and Ne in the sd model space with USDC two body effective interactions with the experimental data in reference (19).

S	ical ıte	data	ıs	ical ıte	data	ıs	ical ıte	data
Nucleus	Theoretical calculate	Exp. da	Nucleus	Theoretical calculate	Exp. da	Nucleus	Theoretical calculate	Exp. d
	Th			Th			Th	<u> </u>
<sup>28</sup> Si	1.1	1.12(0.18)	<sup>24</sup> Mg	1.1	1.08(0.3)	<sup>20</sup> Ne	1.076	1.08(0.08)
<sup>29</sup> Si	-0.522	-	$^{25}$ Mg	-0.897	-0.855(0.08)	<sup>21</sup> Ne	-0.734	-
		0.555(0.03)						0.661(0.005)
$^{30}$ Si	0.756	0.9(0.2)	$^{26}$ Mg	1.925	1(0.3)	<sup>22</sup> Ne	0.78	0.65(0.02)
31Si	0.55		$^{27}$ Mg	-0.396	-	<sup>23</sup> Ne	-1.153	-1.079(0.01)
					0.041(0.0015)			
<sup>32</sup> Si	0.944		$^{28}$ Mg	1.474		<sup>24</sup> Ne	1.733	
<sup>33</sup> Si	1.135		$^{29}$ Mg	0.986	0.978(0.06)	<sup>25</sup> Ne	-0.888	-1(0.001)
<sup>34</sup> Si	2.86		$^{30}$ Mg	2.187		<sup>26</sup> Ne	2.507	
			$^{31}$ Mg	1.348	-0.883(0.015)	<sup>27</sup> Ne	0.794	
			$^{32}$ Mg	3.294		<sup>28</sup> Ne	2.708	
			9			<sup>29</sup> Ne	1.211	
						$^{30}$ Ne	3.65	

**Figure 1** shows more details, where the magnetic moments result for Si, Mg, and Ne isotopes behave differently across all three chains. The theoretical values for <sup>28-34</sup>Si isotopes have a smooth trend with small fluctuations, suggesting mild structural effects. On the other hand, Mg isotopes show an abrupt change at N=19, which suggests the nucleus is entering the Island of Inversion region, reflecting a change in shell structure at this neutron number due to intruder states and configuration mixing. However, Ne isotopes exhibit a consistent and regular behavior in the theoretical results throughout the entire chain, indicating these nuclei possess structural stability and are mostly free from complex configuration mixing.

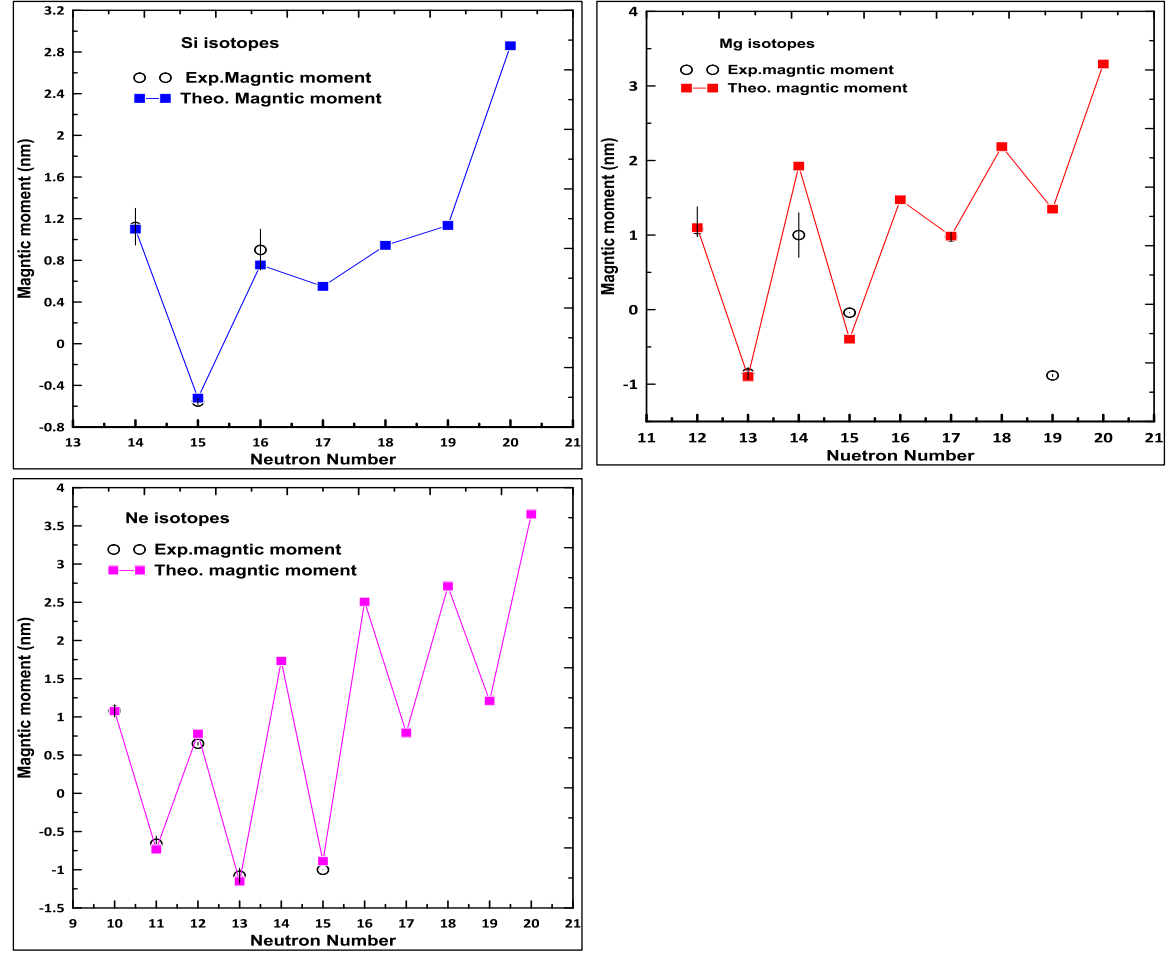


Figure 1. The magnetic dipole moment of Si, Mg, and Ne isotopes with available experimental data (19).

## 3.2. Electric Quadrupole Moments

the calculation and representation of the electric quadrupole moments of Si, Mg, and Ne isotopes were shown in **Table 2** and **Figure 2**. Comparing our electric quadrupole moments calculations for the isotopes to experimental data from Refs (19,20), using two body effective interactions within the sd model space, is shown in **Figure 2**.

**Table 2.** Experimental data from (19, 20) were compared to the calculated electric quadrupole moments in  $e^2 fm2$  for Si, Mg, and Ne isotopes.

Nucleus	Theoretical	Exp.data	Nucleus	Theoretical	Exp.data	Nucleus	Theoretical	Exp.data
	calculate			calculate			calculate	
<sup>28</sup> Si	19.03	16	<sup>24</sup> Mg	-17.58	-29	<sup>20</sup> Ne	-14.31	-23
<sup>29</sup> Si	0		$^{25}$ Mg	20.41	20.1	<sup>21</sup> Ne	10.18	10.1
<sup>30</sup> Si	2.73	-5	$^{26}$ Mg	-13.36	-14	<sup>22</sup> Ne	-14.03	-19
<sup>31</sup> Si	-8.5		$^{27}$ Mg	0		<sup>23</sup> Ne	14.92	14.5
<sup>32</sup> Si	13.53		$^{28}$ Mg	-16.13		<sup>24</sup> Ne	-1.24	
<sup>33</sup> Si	5.91		$^{29}$ Mg	-10.32	-16	<sup>25</sup> Ne	0	
<sup>34</sup> Si	11.1		$^{30}$ Mg	-12.93		<sup>26</sup> Ne	-9.14	
			$^{31}$ Mg	9.3	-29	<sup>27</sup> Ne	-7.73	
			$^{32}$ Mg	-11.12	20.1	<sup>28</sup> Ne	-2.13	
						<sup>29</sup> Ne	7.34	
						<sup>30</sup> Ne	-0.24	

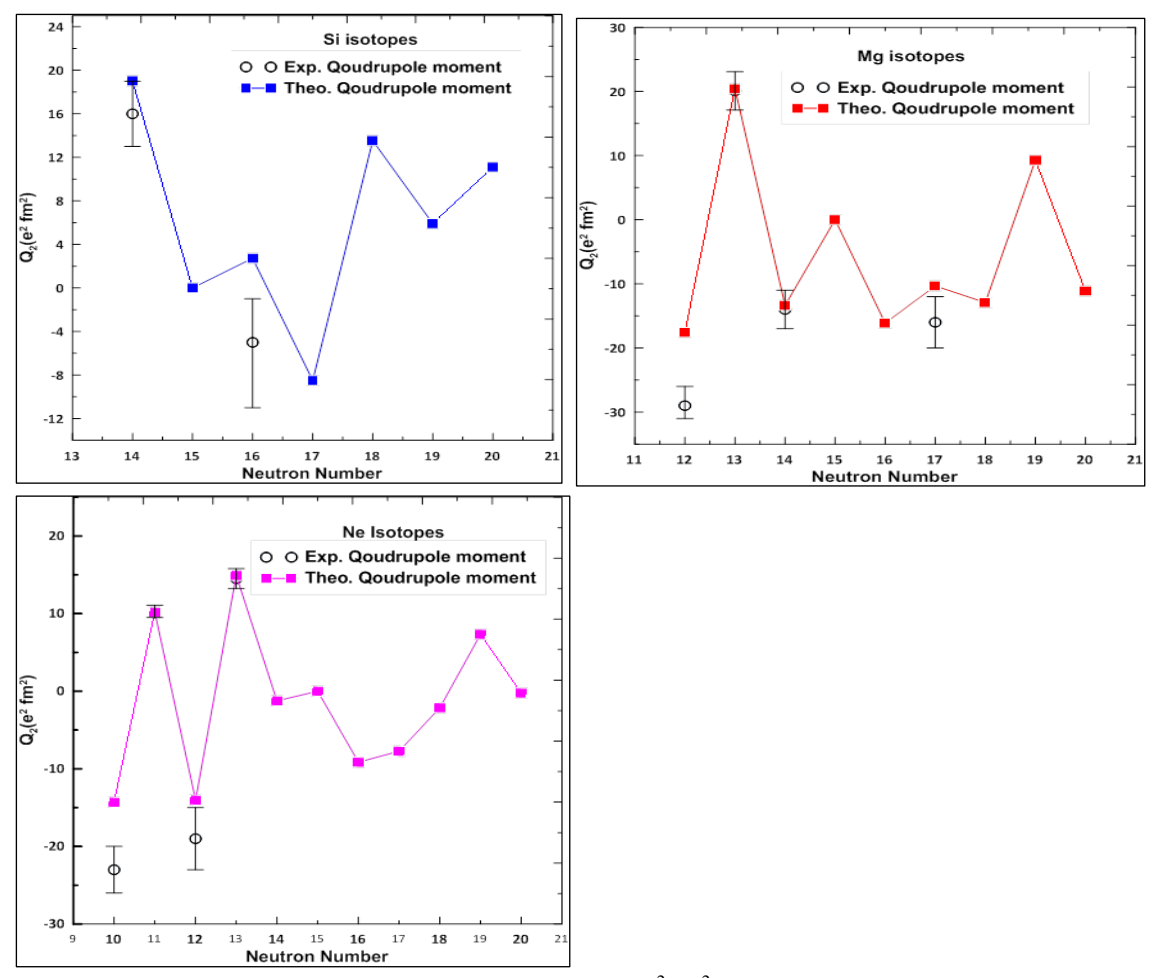


**Figure 2.** The calculated electric quadrupole moments  $Q_2$  ( $e^2$  fm<sup>2</sup>) vs the experimental data (19, 20) for Si, Mg, and Ne isotopes.

Magnesium and odd neon isotopes show there is a reasonable agreement between the theoretical and experimental data, while some disparity exists for even silicon and neon isotopes. This difference is attributed to the nuclear structure where odd isotopes have an unpaired neutron which imparts non-zero angular momentum to the nucleus along with pronounced deformations that theoretical models capture impressively resulting in accurate predictions of the quadrupole moment. Even isotopes, however, having paired neutrons tend to be more towards the spherical shape which makes their quadrupole moments highly sensitive to the details of the model, thereby resulting in less agreement with experimental data.

### 3.3. Reduced deformation parameter $\beta_2$

The behavior of the reduced nuclear deformation parameter  $\beta_2$  as a function of neutron number for Si, Mg, and Ne isotopes were illustrated in **Figure 3**. Theoretical calculations predict a general decrease in  $\beta_2$  with increasing neutron number for these isotopic chains, reflecting a trend toward spherical nuclear shapes as the neutron number approaches the traditional shell closure at N=20. However, experimental data reveal a deviation from this trend, with an unexpected increase in  $\beta_2$  observed at N=20 for Mg isotopes and at N=16 for Ne isotopes. This anomalous behavior suggests a weakening or breakdown of conventional magic numbers, attributed to the intruder states from the fp shell into the sd shell, a hallmark of the NIOI region. In this region, enhanced collectivity and significant shell mixing drive increased nuclear deformation, highlighting the inadequacy of traditional shell models in describing these exotic nuclei.

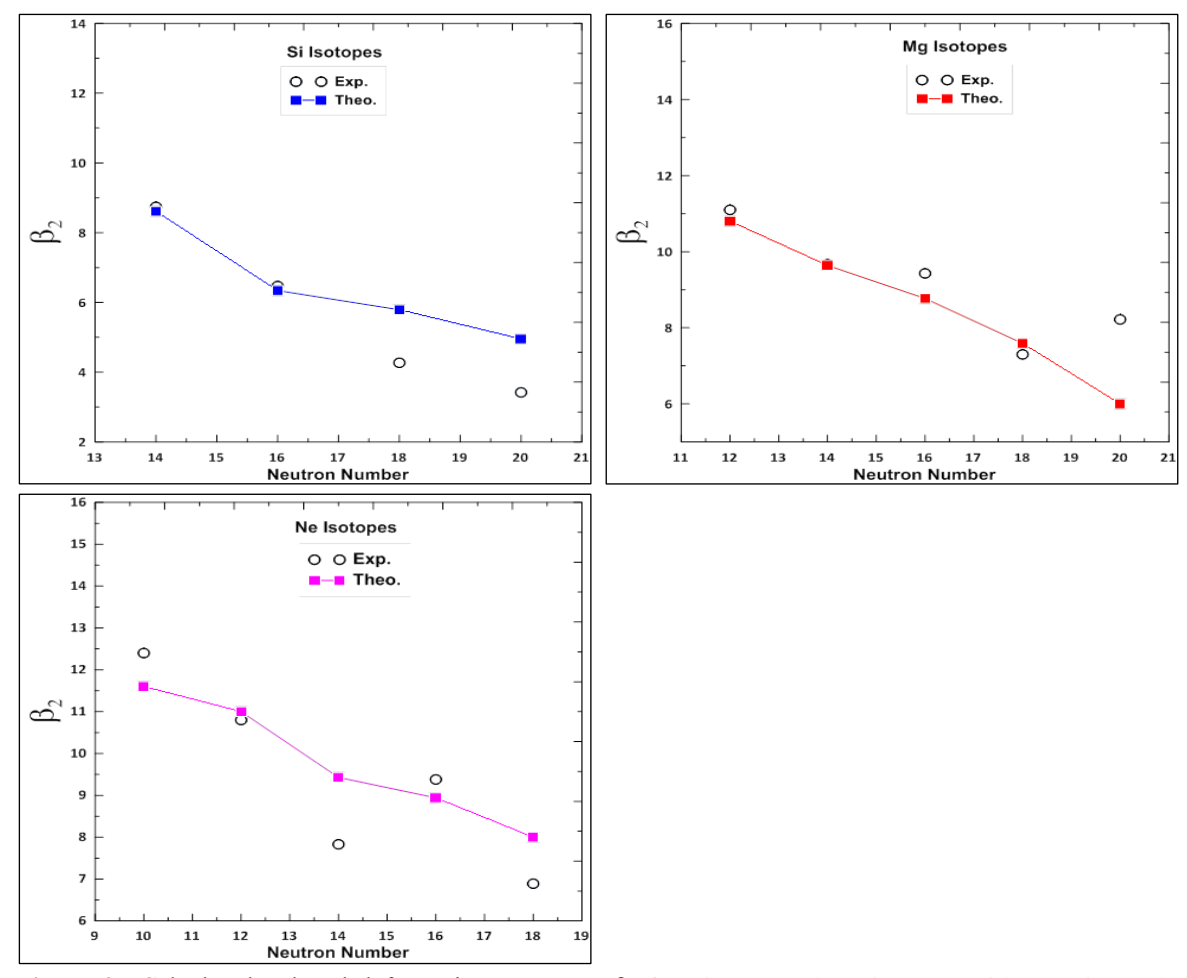


**Figure 3.** Calculated reduced deformation parameter  $\beta_2$  for Si, Mg, and Ne isotopes with experimental data taken from (21-30)

#### 4.Conclusion

In summary, we have investigated the electromagnetic moments and quadrupole deformations as well as the reduced deformation parameter  $\beta_2$  of even-even Ne, Mg, and Si isotopes in and around the island of inversion region using the sd model space and USDC two-body effective interaction. The calculated results appear to match in the light nuclei, but when the number of neutrons increases, while this interaction is generally reliable for typical sd-shell nuclei, it proves inadequate within the island of inversion. The primary reason for this limitation is the reduction of the shell gap and the emergence of intruder configurations. Specifically, the N=20 shell gap diminishes in neutron-rich nuclei, leading to significant structural changes that affect excitation energies and transition probabilities. This leads to significant mixing with intruder states from the fp-shell. Since these interactions do not account for excitations into the fp-shell, they are inadequate for accurately reproducing experimental trends.

## Acknowledgements

We sincerely thank Prof. Dr. B. A. Brown, from Michigan State University, for providing us with the shell model code NuShellX@MSU.

#### **Conflict of Interest**

This article does not contain any conflicts of interest.

#### **Funding**

The article was done depending on self-fund and no establishments supplied us.

#### **Ethical Clearance**

The work and calculations were accomplished using the shell model code NuShellX@MSU (1983) developed by Prof. Dr. B. A. Brown from Michigan State University.

#### References

- 1. Ali AH. Investigation of the quadrupole moment and form factors of some Ca isotopes. Baghdad Sci J. 2020;17(2):18. https://doi.org/10.21123/bsj.2020.17.2.0502
- 2. Wilson GL, Catford WN, Orr NA, Diget CA, Matta A, Hackman G, Williams SJ, Celik IC, Achouri NL, Al Falou H, Ashley R. Shell evolution approaching the N=20 island of inversion: Structure of 26Na. Phys Lett B. 2016;759:417–23. <a href="https://doi.org/10.1016/j.physletb.2016.05.093">https://doi.org/10.1016/j.physletb.2016.05.093</a>
- 3. Ali AH, Idrees MT. Study of deformation parameters (β2, δ) for 18, 20, 22, 24, 26, 28Ne isotopes in sdpf shell. Karbala Int J Mod Sci. 2020;6(1):11. <a href="https://doi.org/10.33640/2405-609X.1376">https://doi.org/10.33640/2405-609X.1376</a>
- 4. Rainwater J. Nuclear energy level argument for a spheroidal nuclear model. Phys Rev. 1950;79(3):432. <a href="https://doi.org/10.1103/PhysRev.79.432">https://doi.org/10.1103/PhysRev.79.432</a>
- 5. Brown BA, Wildenthal BH. Status of the nuclear shell model. Annu Rev Nucl Part Sci. 1988;38(1):29–66.
- 6. Radhi RA, Alzubadi AA, Ali AH. Calculations of the quadrupole moments for some nitrogen isotopes in p and psd shell model spaces using different effective charges. Iraqi J Sci. 2017;58(2B):12. https://doi.org/10.24996/ijs.2017.58.2B.12
- Caurier E, Nowacki F, Poves A. Merging of the islands of inversion at N=20 and N=28. Phys Rev C. 2014;90(1):014302. <a href="https://doi.org/10.1103/PhysRevC.90.014302">https://doi.org/10.1103/PhysRevC.90.014302</a>
- 8. Radhi RA, Alzubadi AA, Rashed EM. Shell model calculations of inelastic electron scattering for positive and negative parity states in 19F. Nucl Phys A. 2016;947:12–25. <a href="https://doi.org/10.1016/j.nuclphysa.2015.12.002">https://doi.org/10.1016/j.nuclphysa.2015.12.002</a>
- 9. Brown BA. The nuclear shell model towards the drip lines. Prog Part Nucl Phys. 2001;47(2):517–99. https://doi.org/10.1016/S0146-6410(01)00159-4
- 10.Kameda D, Ueno H, Asahi K, Takemura M, Yoshimi A, Haseyama T, Uchida M, Shimada K, Nagae D, Kijima G, Arai T. Nuclear moments of neutron-rich 32Al. J Phys Conf. 2006;49(1):138. https://doi.org/10.1088/1742-6596/49/1/030
- 11.Alzubadi AA, Obaid RS. Study of the nuclear deformation of some even—even isotopes using Hartree—Fock—Bogoliubov method (effect of the collective motion). Indian J Phys. 2019;93:75—92. https://doi.org/10.1007/s12648-018-1269-2
- 12.Poves A, Sánchez-Solano J, Caurier E, Nowacki F. Shell model study of the isobaric chains A=50, A=51 and A=52. Nucl Phys A. 2001;694(1-2):157-98. <a href="https://doi.org/10.1016/S0375-9474(01)00967-8">https://doi.org/10.1016/S0375-9474(01)00967-8</a>
- 13.Safronova MS, Safronova UI, Radnaev AG, Campbell CJ, Kuzmich A. Magnetic dipole and electric quadrupole moments of the 229Th nucleus. Phys Rev A. 2013;88(6):060501. https://doi.org/10.1103/PhysRevA.88.060501
- 14.Radhi RA, Alzubadi AA. Study the nuclear form factors of low-lying excited states in nucleus using the shell model with Skyrme effective interaction. Few-Body Syst. 2019;60(3):57. https://doi.org/10.1007/s00601-019-1524-x
- 15.Brussaard PJ, Glaudemans PWM. Shell model applications in nuclear spectroscopy. Amsterdam: North-Holland; 1977. <a href="https://lccn.loc.gov/77007915">https://lccn.loc.gov/77007915</a>
- 16.Brink D, Stancu F. Evolution of nuclear shells with the Skyrme density dependent interaction. Phys Rev C. 2007;75(6):064311. <a href="https://doi.org/10.1103/PhysRevC.75.064311">https://doi.org/10.1103/PhysRevC.75.064311</a>

- 17. Glasmacher T, Brown AB, Chromik M, Cottle P, Fauerbach M, Ibbotson R, Kemper K, Morrissey D, Scheit H, Sklenick D, Steiner M. Collectivity in 44S. Phys Lett B. 1997;395:163–8. https://doi.org/10.1016/S0370-2693(97)00077-4
- 18.Brown BA, Radhi R, Wildenthal BH. Electric quadrupole and hexadecupole nuclear excitations from the perspectives of electron scattering and modern shell-model theory. Phys Rep. 1983;101(5):313–58. https://doi.org/10.1016/0370-1573(83)90001-7
- 19. National Nuclear Data Center. Available from: https://www-nds.iaea.org
- 20.Pritychenko B, Birch M, Singh B, Horoi M. Tables of E2 transition probabilities from the first 2+ states in even—even nuclei. At Data Nucl Data Tables. 2016;107:1–139. https://doi.org/10.1016/j.adt.2015.10.001
- 21. Stone N. Table of nuclear magnetic dipole and electric quadrupole moments. At Data Nucl Data Tables. 2005;90(1):75–176. https://doi.org/10.1016/j.adt.2005.04.001
- 22.Liesem H. Unelastische Elektronenstreuung am 1,78 MeV- und 11,4 MeV-Niveau des Si-28. Z Phys. 1966;196:174–84. https://doi.org/10.1007/BF01326426
- 23.Fewell MP, Kean DC, Spear RH, Zabel TH, Baxter AM, Hinds S. Static quadrupole moment of the first excited state of Si-30. Phys Rev Lett. 1979;43(20):1463. https://doi.org/10.1103/PhysRevLett.43.1463
- 24.Raman S, Nestor CW Jr, Tikkanen P. Transition probability from the ground to the first-excited 2+ state of even—even nuclides. At Data Nucl Data Tables. 2001;78(1):1–28. https://doi.org/10.1006/adnd.2001.0858
- 25.Ibbotson RW, Glasmacher T, Brown BA, Chen L, Chromik MJ, Cottle PD, Fauerbach M, Kemper KW, Morrissey DJ, Scheit H, Thoennessen M. Quadrupole collectivity in 32, 34, 36, 38Si and the N=20 shell closure. Phys Rev Lett. 1998;80(10):2081. https://doi.org/10.1103/PhysRevLett.80.2081
- 26.Khvastunov V, Afanasev N, Afanasev V, Bondaren E, Gulkarov I, Savitski G, Shevchen N. Scattering of high-energy electrons by isotopes Mg-24 and Mg-26. J Nucl Phys USSR. 1971;12(1):5.
- 27. Niedermaier O, Scheit H, Bildstein V, Boie H, Fitting J, von Hahn R, Köck F, Lauer M, Pal UK, Podlech H, Repnow R. Safe Coulomb excitation of Mg-30. Phys Rev Lett. 2005;94(17):172501. https://doi.org/10.1103/PhysRevLett.94.172501
- 28. Pritychenko BV, Glasmacher T, Cottle PD, Fauerbach M, Ibbotson RW, Kemper KW, Maddalena V, Navin A, Ronningen R, Sakharuk A, Scheit H. Role of intruder configurations in 26, 28Ne and 30, 32Mg. Phys Lett B. 1999;461(4):322–8. https://doi.org/10.1016/S0370-2693(99)00850-3
- 29. Singhal RP, Caplan HS, Moreira JR, Drake TE. Inelastic electron scattering from 20, 22Ne. Can J Phys. 1973;51(20):2125–37. https://doi.org/10.1016/0375-9474(75)90525-4
- 30. Niedermaier OT. Thesis. Univ Heidelberg, Germany; 2005.